

## **Role of Kidney Injury Molecule-1 Expression, Wnt Proteins (Beta- catenin) and Endogenous Irisin in a Rat Model of Renal fibrosis: Renoprotective Effect of Metformin**

**Mohamed Adel<sup>1,\*</sup> and Ahmed E. Eladl<sup>2</sup>**

<sup>1</sup>. Department of Medical Physiology, Faculty of Medicine, Mansoura University, Egypt

<sup>2</sup>. Department of Pathology, Faculty of Medicine, Mansoura University, Egypt

**Submit Date:** May 21, 2020  
**Revise Date:** July 2, 2020  
**Available online:** Jan 10, 2021

### **Keywords**

- Renal Fibrosis
- Beta- catenin and Irisin

### **Abstract**

Metformin reduces glucose level and improves insulin sensitivity. Recently, metformin has gained attention for its pleiotropic effects. In this study, we examined the effect of metformin in a rat model of renal fibrosis. Rats were randomly assigned to one of four groups (n = 6/group): 1, control negative: received saline, 2, control positive UUO: rats underwent 14 days UUO and 3, (Metformin + UUO): rats received oral metformin (300 mg/kg/day daily ×21 days). 4, (Metformin +Captopril + UUO): rats were treated by metformin (300 mg/kg/day daily ×21 days) and Captopril (50 mg/Kg/day ×21 days). UUO induced a significant increase in serum creatinine and serum K<sup>+</sup> levels. Also, KIM-1 and Wnt/β-catenin expressions are upregulated after UUO. Metformin led to a significant decrease in serum creatinine level and a significant increase in serum irisin level. Metformin administration attenuated UUO -induced increase in MDA and NOX-4 and increased GSH level. Moreover, metformin led to a significant decrease in KIM-1 expression and Wnt/β-catenin expression in renal tissue. Overall, our results suggest a potential protective role of metformin in UUO -induced renal fibrosis via attenuation of expression of NOX-4, KIM-1 and Wnt/β-catenin and increase serum irisin level.

## INTRODUCTION

Obstructive uropathy, caused by prevention of urine flow, results in renal damage and loss of renal function. The obstruction can occur at any level of the urinary tract. The most common cause of obstruction in adults is urolithiasis, while obstructive nephropathy in children is mostly congenital (1). Acute obstruction of the ureter, rapidly, triggers a cascade of events in the kidneys. First, renal blood flow and the glomerular filtration rate drop. Within few days, hydronephrosis starts to develop, followed by interstitial inflammatory infiltration, apoptosis and necrosis.

The main function of metformin, a biguanide compound widely used for treatment of type 2 diabetes mellitus, is to lower the level of blood glucose (2, 3) by inhibiting hepatic gluconeogenesis (4, 5, 6) and increase cellular glucose uptake (7, 8). Furthermore, metformin may decrease cardiovascular complications for these patients (9, 10). Metformin has, also, been tested in various other disease models where it has been shown to have anti-oncogenic (11, 12), cardioprotective (13, 14), and anti-inflammatory effects (15, 16). Metformin attenuated diabetic nephropathy when tested in a streptozotocin-induced diabetic nephropathy model, possibly by upregulating the anti-oxidative response (17, 18, 19, and 20).

Wnt/ $\beta$ -catenin signaling is a key pathway that regulates cell fate, organ development, tissue homeostasis, as well as, injury and repair. Although relatively silent in normal kidney, Wnt/ $\beta$ -catenin signaling is re-activated after renal injury in a wide variety of kidney disorders. Moreover, multiple components of the renin–angiotensin

system are the direct downstream targets of Wnt/ $\beta$ -catenin.

Irisin was found to convert white fat into brown fat (21). Subsequent studies have confirmed that irisin is involved in a variety of physiological functions, including regulating energy metabolism (22, 23).

Kidney injury molecule-1 (KIM-1) is a type 1 cell membrane glycoprotein composed of six cysteine immunoglobulin-like and mucin domain (18). KIM-1 is normally undetectable in normal urine but it is expressed at high levels following kidney insult. Kidney injury molecule (KIM-1) is a novel biomarker for renal proximal tubular injury (19).

In this study, we investigated the effects of metformin on renal fibrosis induced by obstructive uropathy. We hypothesized that metformin prevents UUO- induced renal fibrosis and increases the anti-oxidant response in obstructive uropathy. We further tested the dependency of these effects on the expression of kidney tubular injury molecule-1 (KIM-1), NADPH oxidase homolog (NOX-4) and Wnt/ $\beta$ -catenin.

We set out therefore to: (i) test the hypothesis that a unilateral obstructive uropathy model can induce renal fibrosis; and, if confirmed, (ii) assess whether the increase in NOX-4, KIM-1 and Wnt/ $\beta$ -catenin expression is involved in renal fibrosis induced by UUO (iii) investigate the possible protective effects of metformin and renin–angiotensin system inhibition by captopril against UUO- induced renal fibrosis (iv) identify the correlation between serum irisin level, serum  $K^+$ , serum creatinine, renal tissue MDA, KIM-1 expression and NOX-4.

## 2. Materials and Methods

### 2.1. Experimental Animals

Twenty four male albino Sprague Dawley rats weighing 180-200 grams were used in the present study. The animals had free access to food and water and were housed in individual cages with a 12-hour light-dark cycle. The animals were adapted to these conditions for at least one week before being used in the experiments and general conditions were monitored throughout the study. All protocols and experimental procedures were approved by the institutional review board (IRB) at Mansoura Faculty of Medicine with approval code R.19.04.490-2019/04/20.

### 2.2. Study Groups

Rats were randomly assigned to one of four groups ( $n = 6/\text{group}$ ): 1, Control negative: sham rats, which were matched according to weight and age, had their ureters dissected free, but the ureters were not occluded, received saline (Sal. group), 2, control positive obstructive uropathy, UUO: rats underwent unilateral ureteral obstruction (UUO) surgery and 3, (Metformin +UUO) rats received oral metformin (300 mg/kg/day daily for 21 days) (17). 4, (Metformin +Captopril +UUO), rats were treated by angiotensin converting enzyme inhibitor (Captopril) (50 mg/Kg/day  $\times$  21 days) (24).

### 2.3. Unilateral ureteral obstruction (UUO) surgery

Through an abdominal incision a silk ligature was tied around the left ureter to make a complete obstruction before closure of the animal. Both pre- and post-surgery the animals received analgesic treatment. Male rats were treated with metformin (Sigma-Aldrich, USA) (300 mg/kg/day) for 21 days. On day 7, the rats underwent UUO and were sacrificed on day 21(25). At the day of sacrifice,

blood was collected directly from the left ventricle of the heart. Blood was centrifuged and serum levels of creatinine, potassium and irisin were measured.

### 2.4. Collection of renal samples

The animals were anesthetized with pentobarbital [0.6 ml/ kg] and the blood collected by heart puncture and allowed to clot for 30 minutes. Serum was separated by centrifugation at 2500 rpm for 15 minutes and used for biochemical estimations. After that rats were sacrificed by cervical dislocation and the abdomen of terminated animal was cut open quickly and the kidney was immediately removed and washed thoroughly with ice-cold saline and dried with filter paper and weighted. The kidneys were then processed for real time polymerase chain reaction (RT-PCR) ( $n = 6$ ). Animals were prepared in parallel for immunohistochemistry. Then portion of the kidney was used to assess biochemical parameters.

### 2.5. Determination of creatinine and $K^+$ in serum

#### 2.5a. Determination of creatinine in serum

The assay is based on the reaction of creatinine with sodium picrate. Creatinine reacts with alkaline picrate forming a red complex. The time interval chosen for measurement avoids interference from other serum constituents. The intensity of the color formed is proportional to creatinine concentration in the plasma (26).

#### 2.5 b. Determination of $K^+$ in serum

Serum samples were separated by centrifugation at 3000 rpm for 15 minutes. The clear serum was received in dry sterile tubes and used directly for determination of  $K^+$  (27).

## 2.6 . Assay of lipid peroxidations marker malondialdehyde (MDA) and antioxidant reduced glutathione (GSH) level in renal tissues

About 50 -100 mg of kidney tissues will be homogenized in 1-2 ml cold buffer (50 mM potassium phosphate, pH 7.5, 1 mM EDTA) using mortar and pestle then centrifuged at 4,000 rpm for 15 minutes at 4°C. The supernatant will be kept at - 20 ° C until it is used for analysis. Malondialdehyde (MDA) and reduced glutathione (GSH) in the supernatant of kidney homogenates were measured using a colorimetric method according to the manufacturer's instructions (Bio-Diagnostics, Dokki, Giza, Egypt).

## 2.7. Determination of serum irisin level

Irisin level was determined by using rat irisin ELISA kit purchased from Kono Biotech Company. Ltd, Zhejiang, China. Purified rat irisin antibody was used to coat microtiter plate wells to make a solid-phase antibody, then irisin was added to wells, combined antibody which with horseradish peroxidase (HRP) labeled goat anti-rat become antibody-antigen-enzyme-antibody complex. After washing completely, 2, 2, 6, 6-tetramethylpiperidine (TMP) substrate was added to obtain blue color. The reaction was terminated by the addition of sulphuric acid solution and the color change is measured spectrophotometrically at a wavelength of 450 nm. The concentration of rat irisin in the sample was then determined by comparing the optical density of the sample to the standard curve. Serum – coagulation at room temperature 10-20 minutes, then centrifugation 20 minutes at the speed of 2000-3000 rotations per minute to remove supernatant, if precipitation appeared, centrifugal again.

## 2.8. Histopathological examination of kidney tissue by Hematoxylin and Eosin

Twenty micrometer-thick sections of kidney slices were stained with hematoxylin and eosin (H&E), and the slides of kidney were stained with hematoxylin for 15 minutes and in HCl alcohol solution for 35 seconds. Then, the sections were immersed with eosin for 10 minutes and 90% ethanol for 40 seconds. After that, the section was examined, and images of the kidney tissue were captured under light microscope.

## 2.9. Histopathological examination of kidney tissue by Masson trichrome staining

The dissected left kidneys were cut into small pieces after its dissection out, kept in fixative (10% neutral buffered formalin) for about one week, washed, dehydrated with alcohol of different grades, then cleared by xylene and embedded in paraffin wax to form a hard block. 5-µm thick sections from a hard block were mounted on glass slides and subjected to the following staining procedures: Masson's Trichrome stain for evaluation of collagen and extracellular matrix (ECM) accumulation and interstitial fibrosis.

## 2.10. Immunohistochemical study of a novel biomarker for the early detection of kidney tubular injury after obstructive uropathy (Wnt/ $\beta$ -catenin)

Serial coronal sections (40 µm) were sliced using a freezing sledge microtome, and a 1:6 series was used for all quantitative immunohistochemistry. Peroxidase-based immunostaining was completed. In brief, following quenching of endogenous peroxidase activity where appropriate (using a solution of 3% hydrogen peroxide/10% methanol in distilled water) and blocking of nonspecific secondary antibody binding (using 3% normal serum in Tris-

buffered saline (TBS) with 0.2% Triton X-100 at room temperature for one hour), sections were incubated overnight at room temperature with the appropriate primary antibody diluted in 1% normal serum in TBS with 0.2% Triton X-100 (polyclonal anti-  $\beta$  - catenin rabbit antibody, Cat#YPA1340, dilution 1:200; Chongqing Biospes Co., Ltd., Chongqing, China).

### 2.11. RNA Extraction and First-strand cDNA synthesis

For all animals, the kidney was removed for RNA extraction under standard sterile surgical method. Total RNA was extracted from kidney tissue using Trizol Reagent [Invitrogen, USA] according to the manufacturer's description and treated with RNase-free DNase to remove any residual genomic DNA. Single stranded cDNAs were synthesized by incubating total RNA [1  $\mu$ g] with Revert Aid H Minus M-MuL V Reverse transcriptase [200 U], oligo-[dT] primer [5  $\mu$ M], Random Hexamer Primer [5  $\mu$ M], dNTPs [1 mM], and Ribo Lock RNase-inhibitor [20 U], for 5 min at 25°C followed by 60 minutes at 42°C in a final volume of 20  $\mu$ l. The reaction was terminated by heating at 70°C for 5 minutes.

### 2.12. Real-time RT-PCR Analysis of KIM-1 Expression

Primers for the KIM-1 gene (NM 173149, forward primer: TGGCACTGTGACATCCTCAGA; reverse primer: GCAACGGACATGCCAACATA) and the house keeping GAPDH gene (NM 017008, forward primer: CCTGGAGAAACCTGCAAGTAT; reverse primer: AGCCCAGGATGCCCTTTAGT) were designed using ABI Primer Express software (Applied Biosystems, Foster City, CA). Total RNA was

reverse transcribed with ABI High-Capacity cDNA Reverse Transcription kit and then subjected to real-time PCR using ABI SYBR green PCR master mix (Applied Biosystems, Cheshire, UK). The cycle time values of KIM-1 were normalized with GAPDH, and the relative differences between control and Cd groups were calculated and expressed as percentage of controls.

### 2.13. Quantitative real-time PCR for kidney oxidative stress marker NADPH oxidase homolog (NOX-4)

Total cellular RNA was extracted from a given cell line with Trizol reagent (Invitrogen). Total cellular RNA (2  $\mu$ g) was isolated from cultured cells and reverse-transcribed using oligo (dT) and M-MLV reverse transcriptase (Promega). The cDNA concentration was adjusted to 100 ng/ml, and PCR was performed using an iQ SYBR Green Supermix (Bio-Rad Laboratories, Hercules, CA, USA) with 5 min of predenaturation at 95°C, followed by 40 cycles of DNA amplification including annealing at 60°C for 30 s and extension at 72°C for 30 s. Assays used the following primer sets: NOX-4, 5'-GGCTGGAGGCATTGGAGTAA-3' (forward) and 5'-CCAGTCATCCAACAGGGTGT-3' (reverse);  $\beta$ -actin, 5'-TCAAGATCATTGCTCCTCTG-3' (forward) and 5'-CTGCTTGCTGATCCACATCTG-3' (reverse). The relative expression of the reverse transcription (RT)-PCR products was determined using the  $\Delta$ Ct method. This method calculates the relative expression using the following equation: fold induction =  $2^{-\Delta Ct}$ , where Ct is the threshold cycle and  $\Delta Ct = (Ct_{\text{gene of interest}} - Ct_{\beta\text{-actin}})$ . Each sample was run in triplicate, and three independent experiments were performed. The mean Ct was used in the  $\Delta$ Ct equation.

### 2.14. Statistical Analysis

Values are presented as the mean (+/-) SD. One-way analyses of variance (ANOVA) were used to compare each molecular variable between control negative (Saline), control positive (UUO), (UUO + Metformin) and (UUO + Metformin+Captopril). When a significant interaction was detected, post-hoc t-tests were used to compare the two groups at different time points. Pearson correlation analyses were used to study the correlations between serum K<sup>+</sup>, serum creatinine, serum irisin, renal tissue MDA, KIM-1 expression and NOX-4 expression in UUO group and the correlations between serum irisin level and the estimated parameters. All data were analyzed using SPSS (SPSS, Sigma Plot Software, Inc, Chicago, IL) program statistical package for social science version 17. Results were considered significant when (P < 0.05).

### 3. Results

#### 3.1. Metformin increases serum irisin level and renal tissue antioxidant GSH level and decreases serum creatinine level and oxidative stress marker MDA in a rat model of renal fibrosis

**Table (1): Effect of UUO, (UUO +Metformin) and (UUO +Metformin + Captopril) on serum creatinine level, serum K<sup>+</sup> level, serum irisin level, malondialdehyde (MDA) and reduced glutathione (GSH) level**

	Sal. group	UUO group	UUO +Metformin group	UUO + Metformin +Captopril group
Serum creatinine (mg %)	0.57 ± 0.08	0.91 ± 0.29*	0.66 ± 0.15#	0.51 ± 0.19#
Serum K <sup>+</sup> (mmol/L.)	4.5±0.2	5.2±0.5*	4.9±0.7	4.7±0.4
Serum irisin level (ng/ml)	60.71± 04.21	58.43 ± 7.11	98.17 ± 9.75#	91.7 ± 11.6#
MDA (nmol/g. renal tissue)	12.7±0.47	23.9±0.4*	17.9±0.9*#	14.9±0.8*#
GSH (nmol/g. renal tissue)	112.93± 7.22	54.63*	107.29#	100.43*#

Test used: ANOVA followed by posthoc Tukey for multiple comparisons. Values are expressed as mean ± S.D. (n = 6). \*(P < 0.05): significant in proportional to control. # (P < 0.05): significant as compared with UUO.

#### 3.2. The Effects of UUO, Metformin and captopril on morphology of tubular cells

Kidney sections from UUO group (Figure 1 B) showed irregular arrangement of cells with a

Obstructive uropathy led to a significant increase in serum creatinine in proportional to control (Table 1). While it decreased, significantly, in (UUO + Metformin) and (UUO + Metformin+Captopril) - treated groups. In addition, UUO led to a significant increase in serum K<sup>+</sup> level. While it decreased, significantly, in metformin and (Metformin+Captopril) treated groups in proportional to UUO group. In addition, serum irisin level increased, significantly, in (UUO + Metformin) and (UUO + Metformin+Captopril) treated groups. Moreover, UUO led to a highly significant increase in malondialdehyde (MDA) in proportional to control. While it decreased, significantly, in (UUO + Metformin) and (UUO + Metformin+Captopril) treated groups in proportional to UUO group. Moreover, UUO led to a significant decrease in GSH level in proportional to control. While it increased, significantly, in metformin and (Metformin+Captopril) - treated groups in proportional to UUO group.

reduction in the number of cells, and the cells showed pyknosis (Darkly-stained nucleus and cytoplasm). The number of abnormal cells was significantly reduced in the kidney tissues



obtained from (Metformin + UUO) group (Figure 1 C) and (Metformin + captopril +UUO) group (Figure 1 D).

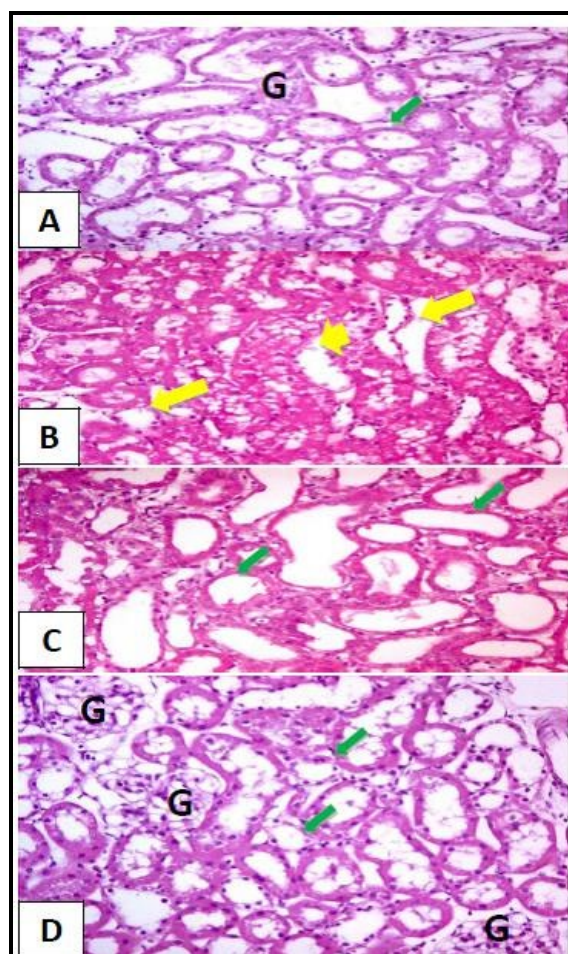


**Figure (1):** Histopathological examination of the renal tubules. **A)** H&E staining of control group (n=6) (H&E, 200 X) showed a normal appearance for kidney tissue. **B)** H&E staining of UUO group (n=6) (H&E, 200 X): swollen proximal tubules epithelial lining with loss of brush border, even the tubules lumen is very narrow due to the swollen epithelial lining (arrowhead). **C)** H&E staining of Metformin + UUO group (n=6) (H&E, 200 X): Metformin administration attenuated renal injury induced by UUO. **D)** H&E staining of the UUO + Metformin + Captopril group (n=6) (H&E, 200 X): metformin and captopril administration attenuated tubular injury induced by UUO.

### 3.3. Metformin and captopril administration attenuated fibrosis in obstructed kidneys

Masson's trichrome staining showed that collagen deposition increased in the interstitial area, suggesting that 14 days UUO induced renal interstitial fibrosis (Figure 2 B). Metformin

treatment significantly attenuated UUO-induced collagen deposition (Figure 2 C). Moreover, metformin and captopril treatment significantly attenuated UUO-induced collagen deposition (Figure 2 D).

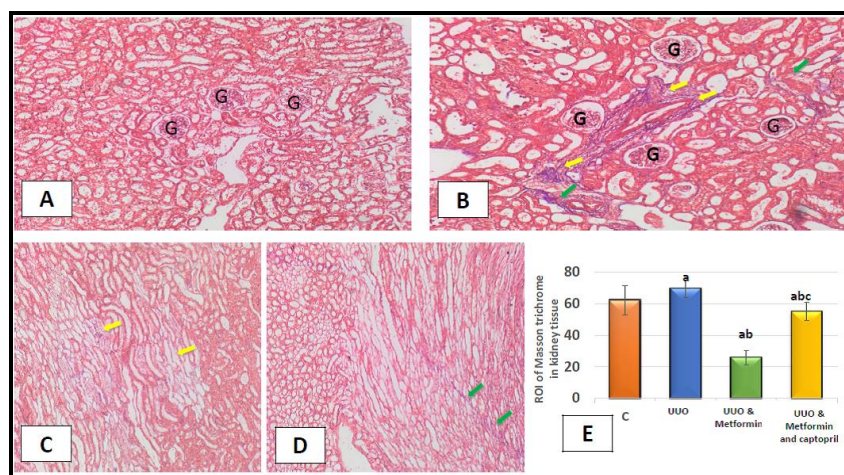


**Figure (2):** Effect of metformin and captopril on collagen production in unilateral ureteral obstruction rats. Representative sections of Masson's trichrome-stained kidneys. Collagen was stained blue. **A)** Masson trichrome staining of the Sal group (n=6): showed a normal appearance for kidney tissue with no evidence of fibrosis (Masson trichrome  $\times 100$ ) **B)** Masson trichrome staining of UUO group (n=6): Masson's trichrome stain shows marked fibrosis (Arrowhead) (Masson trichrome  $\times 100$ ) **C)** Masson trichrome staining of UUO + metformin (n=6): Masson's trichrome stain showed mild degree of fibrosis (Arrow head) (Masson trichrome  $\times 100$ ) **D)** Masson trichrome staining of UUO+ Metformin + Angiotensin converting enzyme inhibitor (Captopril) (n=6): showed mild degree of fibrosis (Arrowhead). **E)** ROI of Masson trichrome staining of kidney tissues

a: significance as compared to control group.

b: significance as compared to UUO group.

c: significance as compared to (UUO +Metformin).

### 3.4. Effect of metformin and captopril on the level of expression of tubular injury marker Wnt/ $\beta$ -catenin in response to 14 days UUO

Figure (3 B) showed that the tubules were significantly dilated in obstructive uropathy group

with increased expression of endogenous Wnt/ $\beta$ -catenin. While its expression decreased in kidney tissues obtained from metformin treated group (Figure 3 C) and kidney tissues obtained from captopril + metformin treated group (Figure 3 D).

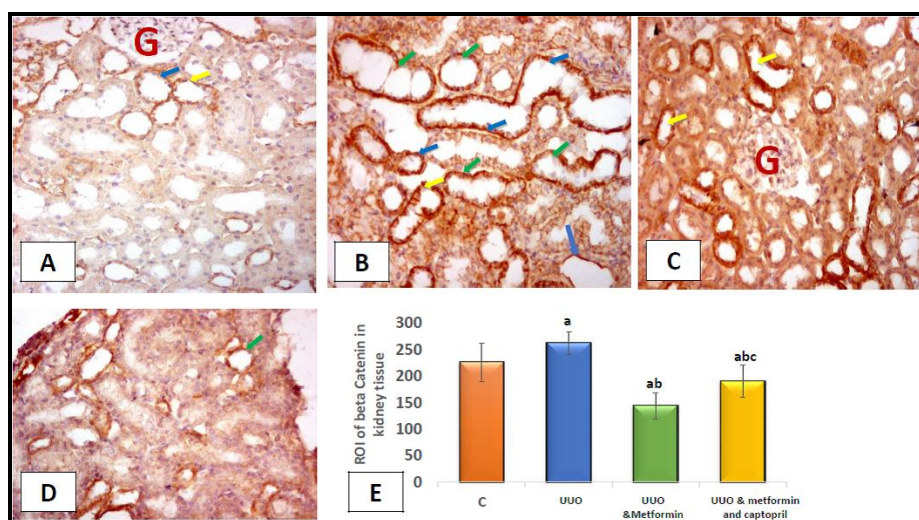


**Figure (3):** Enhanced expressed Wnt/ $\beta$ -catenin was localized in both the injured proximal and distal tubules following UUO. Histopathological examination of renal tubules. **A)** Immunostaining of control group (n=6): showed decreased endogenous Wnt/ $\beta$ -catenin, brown stain (arrowhead) (Magnification, 200X) **B)** Immunostaining of UUO group (n=6): showed increased endogenous Wnt/ $\beta$ -catenin, brown stain (arrowhead) (Magnification, 200X) **C)** Metformin administration led to a significant decrease in the biomarker of kidney injury (Wnt/ $\beta$ -catenin) (Magnification, 200X). **D)** Captopril and metformin administration led to a significant decrease in the biomarker of kidney injury (Wnt/ $\beta$ -catenin) (Magnification, 200X) **E)** ROI of beta- Catenin staining of kidney tissues

a: significance as compared to control group.

b: significance as compared to UUO group.

c: significance as compared to (UUO +Metformin).



### 3.5. Effect of metformin on kidney tubular injury molecule-1 (KIM-1) expression in response to 14 days obstructive uropathy

Figure (4) showed that KIM-1 mRNA and protein expression increased in rats subjected to

obstructive uropathy compared to sal. group. Metformin and captopril treatment attenuated the increased expression of KIM-1 at the mRNA and protein levels, significantly, as compared with UUO.

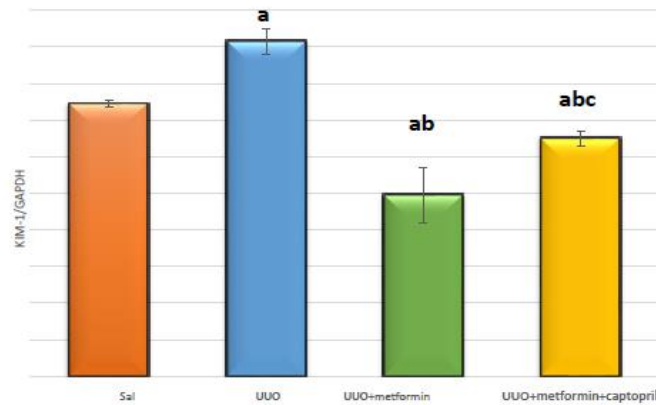


**Figure (4):** Products of RT-PCR for KIM-1 in Sal. control group [1], UUO group [2], Metformin +UUO group [3] and UUO +Metformin +Captopril [4]

**a:** significance as compared to sal. group.

**b:** significance as compared to UUO group.

**c:** significance as compared to (UUO +Metformin).

**Sal:** saline **UUO:** Unilateral ureteral obstruction

### 3.6. Effect of metformin on NADPH oxidase homolog (NOX-4) expression in response to 14 days obstructive uropathy

Figure (5) showed that NOX-4 mRNA and protein expression increased, significantly, in rats subjected to 14 days obstructive uropathy compared to sal. group. Metformin and captopril

treatment attenuated the increased expression of NOX-4 at the mRNA and protein levels, significantly, as compared with UUO.

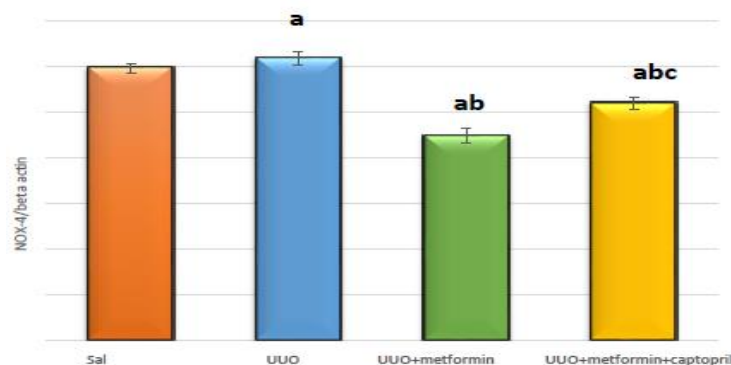


**Figure (5):** Products of RT-PCR for NOX-4 mRNA and protein expression in sal. control group [1], UUO group [2], Metformin +UUO group [3] and UUO +Metformin +Captopril [4].

**a:** significance as compared to Sal. group.

**b:** significance as compared to UUO group.

**c:** significance as compared to (UUO +Metformin).

**Sal:** saline **UUO:** Unilateral ureteral obstruction

3.7. Correlations between serum  $K^+$ , serum creatinine, serum irisin, renal tissue MDA, KIM-1 expression and NOX-4 expression in renal tubules in obstructive uropathy group

Table (2) showed that there are a significant positive correlations between serum  $K^+$ , serum

creatinine, renal tissue MDA, renal tissue KIM-1, renal tissue NOX-4 expressions and there is a negative correlation with serum irisin level.

**Table (2):** Correlations between serum  $K^+$ , serum creatinine, serum irisin level, renal tissue MDA and kidney tubular injury molecule-1 (KIM-1) expression and NADPH oxidase homolog NOX-4 expression in obstructive uropathy group (UUO)

Parameters		Serum $K^+$	Serum Creatinine	Serum irisin	Renal tissue MDA	KIM-1 expression	NOX-4
Serum $K^+$	r		0.9	-0.4	0.8	0.8	0.998
	p		0.000***		0.000***	0.000***	
Serum Creatinine	r			0.1	0.5	0.4	0.375
	p			-0.3	0.013*	0.023*	0.000***
Serum irisin	r			0.2	-0.6	-0.1	0.071
	p				0.8	0.5	-0.2
Renal tissue MDA	r					0.8	0.5
	p					0.000***	0.299
KIM-1 expression	r						0.155
	p						0.958
NOX-4	r						0.000***
	p						

KIM-1: Kidney Tubular Injury Molecule-1.

NOX-4: NADPH Oxidase Homolog 4.

r: Pearson's correlation coefficient.

P: Probability.

\*(P < 0.05): is considered significant.

\*\* \* (P < 0.001): is considered highly significant.

**Table (3):** The correlation between serum irisin level and the estimated parameters

	Sal.		UUO		UUO + Metformin		UUO + Metformin + Captopril	
	Level of irisin ( ng\ ml)		Level of irisin ( ng\ ml)		Level of irisin ( ng\ ml)		Level of irisin ( ng\ ml)	
	r	P	r	P	r	P	r	P
Serum $K^+$	-0.514	0.010*	-0.910	.000***	-0.830	.000***	-0.801	.000***
Serum Creatinine	-0.464	0.022*	-0.860	.000***	-0.471	0.020*	-0.474	0.019*
Renal tissue MDA	-0.460	0.024*	-0.890	.000***	-0.811	.000***	-0.768	.000***
Renal tissue GSH	0.453	0.0026*	0.542	0.006*	0.035	0.871	0.420	0.041*
KIM-1 expression	-0.473	0.020*	-0.888	.000***	-0.822	.000***	-0.771	.000***
NOX-4	-0.442	0.030*	-0.806	.000***	-0.467	0.022*	-0.497	0.013*

r: Pearson's correlation coefficient

P: Probability

\*(P < 0.05): is considered significant.

\*\* \* (P < 0.001): is considered highly significant.

### 3.8. Correlations between serum irisin level and the estimated parameters

Table (3) showed that there are negative correlations between serum irisin level and serum  $K^+$ , serum creatinine, renal tissue MDA, KIM-1 expression and NOX-4. However, serum irisin level shows a positive correlation with renal tissue antioxidant GSH level.

## 4. Discussion

The main findings in the present study are: (a) obstructive uropathy increased serum creatinine and serum  $K^+$ , significantly, in proportional to control (b) Wnt/ $\beta$ -catenin and KIM-1 expressions were upregulated in the injured renal tubules in obstructive uropathy group (c) metformin administration led to a significant decrease in serum creatinine, serum  $K^+$ , Wnt/ $\beta$ -catenin and KIM-1 expression in proportional to obstructive uropathy. (d) angiotensin converting enzyme inhibitor (Captopril) and metformin led to a significant decrease in serum creatinine, serum  $K^+$  level, KIM-1 expression and  $\beta$ -catenin expression in proportional to obstructive uropathy (e) metformin increased both GSH levels in rats subjected to obstructive uropathy, indicating that metformin upregulates the antioxidative response to obstructive uropathy (f) metformin increases serum irisin level in a rat model of obstructive uropathy

Reactive oxygen species are a recently recognized mechanism in the pathogenesis of obstructive uropathy in experimental models (28). So, we decided to measure MDA and GSH levels as biomarkers of oxidative stress in renal tissue. In this study, we confirmed the protective role of metformin on renal tissue damage after the

induction of obstructive uropathy in rats. Our results showed that the obstructed kidney had significantly higher tissue MDA, and lower GSH levels along with more fibrosis. Our findings corroborate those of earlier studies demonstrating that an enhanced endogenous oxidative stress has a major role in the severity of obstructive uropathy - induced acute renal failure (29, 30).

Renal fibrosis underlies all forms of end-stage kidney disease, regardless of the primary insult. It is characterized by the excessive accumulation of extracellular matrix components after renal injury, which eventually leads to renal failure (31). Currently, treatment of renal fibrosis is severely limited and often ineffective (32, 33). Kidney transplantation is the only effective option for end-stage renal fibrosis. However, limited organ availability and the high morbidity of transplantation highlight the urgent need for novel strategies to prevent renal fibrosis. Metformin is the most frequently prescribed antidiabetic drug worldwide. It has been prescribed to patients with type 2 diabetes, yet its underlying mechanism remains largely elusive (30). Metformin reduces glucose levels and improves insulin sensitivity. Recently, metformin has gained attention for its pleiotropic effects. In this study, we examined the effect of metformin on renal fibrosis.

The animal model used in our study was the obstructive uropathy model, a well-established model of renal fibrosis. The pathogenesis of renal fibrosis caused by obstructive uropathy involves infiltration of the kidney by inflammatory cells including monocytes, activation and possible transformation of intrinsic renal cells, and interactions between infiltrating and resident cells (27). This is in agreement with our results which

showed that obstructive uropathy induced renal fibrosis as indicated by the upregulation of extracellular matrix proteins and collagen deposition in the kidney sections stained by Masson's trichrome staining.

In this study, metformin treatment significantly attenuated UUO-induced collagen deposition and attenuated renal fibrosis. This is in agreement with the previous finding that metformin attenuated progression of fibrosis in dogs subjected to 14 days unilateral ureteral obstruction (17), as well as, in mouse models of 7 and 14 days obstructive uropathy (18, 19).

Activation of the renin-angiotensin system is associated with various deleterious effects, including vasoconstriction, inflammation, hypertrophy, and extracellular matrix protein synthesis (34, 35, 36). Angiotensin II, the main effector of the renin-angiotensin system, is a critical mediator of fibrogenesis. We used the UUO model, also, to detect the role of RAS inhibition in renal fibrosis. In the present study, inhibition of renin-angiotensin system by captopril attenuated renal fibrosis. In agreement with the previous finding that angiotensin II was upregulated in the kidney tissue of UUO rats, accompanied by the upregulation of angiotensin II receptors, suggesting that the renin-angiotensin system had been activated and TGF-beta is the key factor of the profibrotic effects of angiotensin II (37).

Whereas some data point to a protective role of Wnt/ $\beta$ -catenin in healing and repair after acute kidney injury, increasing evidence suggests that sustained activation of Wnt/ $\beta$ -catenin is associated with the development and progression of renal fibrotic lesions. Here, in this study, kidney

sections obtained from obstructive uropathy group showed increased expression of endogenous Wnt/ $\beta$ -catenin. Its expression decreased in kidney tissues obtained from metformin - treated group and kidney tissues obtained from inhibitor of renin-angiotensin system captopril-metformin treated group. This is in agreement with the previous findings that in kidney cells, Wnt/ $\beta$ -catenin promotes the expression of numerous fibrosis-related genes, such as snail1, plasminogen activator inhibitor-1, and matrix metalloproteinase-7 (38).

Antioxidants can ameliorate obstructive uropathy -associated injury, as previously demonstrated that the antioxidants NADPH oxidase inhibitor diphenyleneiodonium and the complex I inhibitor rotenone prevented renal damage in response to 3 days obstructive uropathy (39, 340, 41). Our current data suggest that metformin can upregulate GSH activity, which might reduce ROS in response to obstructive nephropathy. Also, our current data showed that metformin attenuated MDA in the renal tissue. So, metformin acts as an antioxidant has an essential role in reducing levels of reactive oxidant species (ROS) produced during obstructive uropathy, limiting the damage created by ROS.

Also, in the present study, we used the model to answer the question of whether KIM-1 was actually playing a role in fibrosis, whether it was simply a biomarker of injury, or if alternatively it was driving a fibrotic reaction when expressed? KIM-1 has been demonstrated to be a proximal tubular injury marker (42, 43). In the present study, we demonstrated a downregulation of KIM-1 in the metformin-treated rats. Also, we demonstrated a downregulation of KIM-1 in



(metformin+captopril)- treated rats. In agreement with the finding that KIM-1 expression was strongly upregulated two days after unilateral ureteral obstruction (44). In this genetic approach, there is activation of expression of KIM-1 in kidney tubules in the absence of any other injury stimulus (44). Also, in this transgenic model, expression of KIM-1 caused spontaneous and progressive interstitial kidney inflammation and fibrosis, even in the absence of any kidney injury. This finding was indicative of a role for KIM-1 in fibrosis. Also, in this genetic approach (44), a mouse model with a truncated form of KIM-1, the mice were protected from fibrosis. Furthermore, expression of KIM-1 was associated with upregulation of the proinflammatory cytokine monocyte chemoattractant protein-1 (MCP-1).

Here, we found that metformin increased serum irisin level in obstructive uropathy. This finding is in agreement with Li et al. (2015) (45) who found that metformin significantly elevated plasma irisin levels in WT and in db/db mice. In addition, it could be hypothesized that prevention or attenuation of renal tissue oxidative stress after UUO and the significant increases in serum irisin level contributes to prevent UUO-induced renal fibrosis. This hypothesis is supported by several studies showing that irisin acts as a therapeutic agent that inhibits oxidative stress and fibrosis (46) and recently, it was reported that irisin can alleviate the occurrence of heart, liver and kidney fibrosis (47,48,49). Also, in the present study, metformin decreased serum creatinine and  $K^+$  level. We assessed expression of NOX-4, KIM-1 and Wnt/ $\beta$ -catenin and serum irisin level to answer the question of whether there is a correlation between antifibrotic effect of metformin and its

renoprotective effect? Metformin protects against renal fibrosis via its antioxidative effect via attenuation of expression of NOX-4 and MDA and via stimulation of endogenous irisin release, as well as, its renoprotective effect via attenuation of expression of KIM-1 and Wnt/ $\beta$ -catenin.

## 5. Conclusions

Here, in the present study, inhibition of KIM-1, NOX-4, Wnt/ $\beta$ -catenin expression and increased serum irisin level by administration of metformin and inhibition of renin-angiotensin system by captopril alleviate kidney fibrosis induced by UUO. Thus, our data provide a rationale for the treatment of renal fibrosis using metformin and captopril. We believe the current study is an important step towards the further development of irisin as a novel therapeutic approach for kidney fibrosis.

## Acknowledgement

Mansoura experimental research center (MERC) is acknowledged for its contribution to the experimental part of the study.

**Author Contributions: Mohamed Adel:** shared in the idea, the induction of UUO model, biochemical analysis, data analysis and paper writing. **Ahmed El Adl:** shared in the induction of UUO model and histopathological examination

## References

1. Zecher M, Guichard C, Velasquez MJ, Figueroa G, Rodrigo R. 2009. Implications of oxidative stress in the pathophysiology of obstructive uropathy. *Urol Res.* 37:19-26.
2. Bailey, C. J. & Turner, R. C. 1987. Metformin. *Am. J. Hosp. Pharm.* 334, 574–579.

3. **DeFronzo, R. A., Eldor, R. & Abdul-Ghani, M.** 2013. Pathophysiologic approach to therapy in patients with newly diagnosed type 2 diabetes. *Diabetes Care* 36, 127–138.
4. **Kim, Y. D.** 2008. Metformin Inhibits Hepatic Gluconeogenesis Through AMP-Activated Protein Kinase-Dependent Regulation of the Orphan Nuclear Receptor SHP. *Diabetes*. 57, 306–314.
5. **Foretz, M.** 2010. Metformin inhibits hepatic gluconeogenesis in mice independently of the LKB1/AMPK pathway via a decrease in hepatic energy state. *J. Clin. Invest.* 120, 2355–2369.
6. **Duca, F. A.** 2015. Metformin activates a duodenal Ampk-dependent pathway to lower hepatic glucose production in rats. *Nat. Med.* 21, 506–511.
7. **Galuska, D., Nolte, L. A., Zierath, J. R. & Henriksson, H. W.** 1994. Effect of metformin on insulin-stimulated glucose transport in isolated skeletal muscle obtained from patients with NIDDM. *Diabetologia* 37, 826–832.
8. **Hundal, H. S., Ramlal, T., Reyes, R., Leiter, L. A. & Klip, A.** 1992. Cellular Mechanism of Metformin Action Involves Glucose Transporter Translocation from an Intracellular Pool to Plasma Membrane in L6 Muscle Cells. *Endocrinology* 131, 1165–1173.
9. **Lamanna, C., Monami, M., Marchionni, N. & Mannucci, E.** 2011. Effect of metformin on cardiovascular event and mortality: a meta-analysis of randomized clinical trials. *Diabetes, Obes. Metab.* 13, 221–228.
10. **UKPDS.** 1998. Effects of Intensive blood glucose control with metformin on complications in overweight patients with type 2 diabetes (UKPDS 34). *Lancet* 352, 854–865.
11. **Hirsch, H. A., Iliopoulos, D., Tsiachlis, P. N. & Struhl, K.** 2009. Metformin selectively targets cancer stem cells, and acts together with chemotherapy to block tumor growth and prolong remission. *Cancer Res.* 69, 7507–7511.
12. **Buzzai, M.** 2007. Systemic Treatment with the Antidiabetic Drug Metformin Selectively impairs p53-deficient Tumor Cell Growth. *Cancer Res.* 67, 6745–6752.
13. **Gundewar, S.** 2009. Activation of AMP-activated protein kinase by metformin improves left ventricular function and survival in heart failure. *Circ. Res.* 104, 403–411.
14. **Calvert, J. W.** 2008. Acute metformin therapy confers cardioprotection against myocardial infarction via AMPK-eNOS-mediated signaling. *Diabetes* 57, 696–705.
15. **Kalariya, N. M., Shoeb, M., Ansari, N. H., Srivastava, S. K. & Ramana, K. V.** 2012. Antidiabetic drug metformin suppresses endotoxin-induced uveitis in rats. *Immunol. Microbiol.* 53, 3431–3440.
16. **Martin-Montalvo, A.** 2013. Metformin improves healthspan and lifespan in mice. *Nat. Commun.* 4, 2192.
17. **Alhaider, A.** 2011. Metformin attenuates streptozotocin-induced diabetic nephropathy in rats through modulation of oxidative stress genes expression. *Chem. Biol. Interact.* 192, 233–242.
18. **Garamaleki, M. N., Kazemi, D., Heydarinegad, H. & Safarmashaei, S.** 2012. Effect of Metformine (Glucophage) on Renal Function after Complete Unilateral Ureteral

- Obstruction in Dog. *Am. J. Toxicol. Sci.* 4, 6–10.
19. **Kim, H.** 2015. Activation of AMP-activated protein kinase inhibits ER stress and renal fibrosis. *Am. J. Physiol. - Ren. Physiol.* 308, 226–236.
20. **Cavaglieri, R. C., Day, R. T., Feliers, D. & Abboud, H. E.** 2015. Metformin prevents renal interstitial fibrosis in mice with unilateral ureteral obstruction. *Mol. Cell. Endocrinol.* 412, 116–122.
21. **G.E. Maalouf, D. El Khoury,** 2019. Exercise-induced irisin, the fat Browning Myokine, as a potential anticancer agent, *J. Obes.* 6561726.
22. **M.M. Reza.** 2017. Irisin is a pro-myogenic factor that induces skeletal muscle hypertrophy and rescues denervation-induced atrophy, *Nat. Commun.* 8, 1104.
23. **N. Perakakis.** 2017. Physiology and role of irisin in glucose homeostasis, *Nat. Rev. Endocrinol.* 13, 324–337.
24. **Pompermayer K, Amaral FA, Fagundes CT, Vieira AT, Cunha FQ, Teixeira MM, Souza DG.** 2007. Effects of the treatment with glibenclamide, an ATP-sensitive potassium channel blocker, on intestinal ischemia and reperfusion injury. *Eur J Pharmacol.* 556 (1–3):215–222.
25. **Chevalier RL, Forbes MS and Thornhill BA.** 2009. Ureteral obstruction as a model of renal interstitial fibrosis and obstructive nephropathy. *Kidney Int*; 75: 1145-1152.
26. **Murray RL.** 1984. Clin chem. St Louis, Toronto, Princeton: *The C.V. Mosby Co.*;pp. 1261–1266; 418
27. **Berry MN, Mazzachi RD, Rajakovic M.** 1989. Enzymatic determination of potassium in serum. *Clin Chem*; 35:817–820.
28. **Kinugasa F, Noto T, Matsuoka H, Urano Y, Sudo Y, Takakura S.** 2010. Prevention of renal interstitial fibrosis via histone deacetylase inhibition in rats with unilateral ureteral obstruction. *Transpl Immunol.* 23:18–23.
29. **Jiang D, Zhang Y, Yang M, Wang S, Jiang Z, Li Z.** 2014. Exogenous hydrogen sulfide prevents kidney damage following unilateral ureteral obstruction. *Neurourol Urodyn.* 33:538–43.
30. **Martinez-Salgado C, Lopez-Hernandez FJ, Lopez-Novoa JM.** 2007. Glomerular nephrotoxicity of aminoglycosides. *Toxicol Appl Pharmacol.* 223: 86–98.
31. **Campanholle, G.; Ligresti, G.; Gharib, S.A.; Duffield, J.S.** 2013. Cellular mechanisms of tissue fibrosis. 3. Novel mechanisms of kidney fibrosis. *Am. J. Physiol. Cell Physiol.* 304, C591–C603.
32. **Leung, K.C.; Tonelli, M.; James, M.T.** 2013. Chronic kidney disease following acute kidney injury-risk and outcomes. *Nat. Rev. Nephrol.* 9, 77–85.
33. **Decleves, A.E.; Sharma, K.** 2014. Novel targets of antifibrotic and anti-inflammatory treatment in CKD. *Nat. Rev. Nephrol.* 10, 257–267.
34. **Foretz, M.; Guigas, B.; Bertrand, L.; Pollak, M.; Viollet, B.** 2014. Metformin: From mechanisms of action to therapies. *Cell Metab.* 20, 953–966.
35. **.Simoes, E.S.A.; Silveira, K.D.; Ferreira, A.J.; Teixeira, M.M.** 2013. ACE2, angiotensin-(1–7) and Mas receptor axis in

- inflammation and fibrosis. *Br. J. Pharmacol.* 169, 477–492.
36. **Belmadani, S.; Zerfaoui, M.; Boulares, H.A.; Palen, D.I.; Matrougui, K. Microvessel.** 2008. Vascular smooth muscle cells contribute to collagen type I deposition through ERK1/2 MAP kinase, and TGF in response to ANG II and high glucose. *Am. J. Physiol. Heart Circ. Physiol.* 295, H69–H76.
  37. **Yu, L.; Border, W.A.; Anderson, I.; McCourt, M.; Huang, Y.; Noble, N.A.** 2004. Combining TGF-beta inhibition and angiotensin II blockade results in enhanced antifibrotic effect. *Kidney Int.* 66, 1774–1784.
  38. **He W, Dai C, Li Y.** 2009. Wnt/beta-catenin signaling promotes renal interstitial fibrosis. *J Am Soc Nephrol.*; 20: 765–776.
  39. **Tomic, T.** 2011. Metformin inhibits melanoma development through autophagy and apoptosis mechanisms. *Cell Death Dis.* 2, e199.
  40. **Sahra, B. I.** 2010. Targeting Cancer Cell Metabolism: The Combination of Metformin and 2-Deoxyglucose Induces p53-Dependent Apoptosis in Prostate Cancer Cells. *Cancer Res.* 70, 2465–2475.
  41. **Jung, H. H.** 2011. Protective role of antidiabetic drug metformin against gentamicin induced apoptosis in auditory cell line. *Hear. Res.* 282, 92–96.
  42. **Han, W. K., Bailly, V., Abichandoni, R., Thadani, R. & Bonventre, J.** 2002. Kidney Injury Molecule (KIM-1): a novel biomarker for human renal proximal tubular injury. *Kidney Int.* 62, 237–244.
  43. **Ostergaard, M.** 2014. ROS dependence of cyclooxygenase-2 induction in rats subjected to unilateral ureteral obstruction. *Am. J. Physiol. Renal Physiol.* 306, F259–F270.
  44. **Humphreys, B. D.** 2013. Chronic epithelial kidney injury molecule-1 expression causes murine kidney fibrosis. *J Clin Invest.*;123(9):4023–4035.
  45. **D.-J. Li, F. Huang, W.-J. Lu, G.-J. Jiang, Y.-P. Deng and F.-M. Shen.** 2015. Metformin promotes irisin release from murine skeletal muscle independently of AMP-activated protein kinase activation. *Acta Physiol.* 213, 711–721.
  46. **Yifan Rena,b, Jia Zhanga,b, Mengzhou Wanga,b, Jianbin Bia,b, Tao Wanga,b, Minglong Qiuc, Yi Lva,b, Zheng Wub,, Rongqian Wua.** 2020. Identification of irisin as a therapeutic agent that inhibits oxidative stress and fibrosis in a murine model of chronic pancreatitis. *Biomedicine & Pharmacotherapy.* 126, 110101.
  47. **S. Petta.** 2017. Fibronectin type III domain-containing protein 5 rs3480 A&G polymorphism, Irisin, and liver fibrosis in patients with nonalcoholic fatty liver disease. *J. Clin. Endocrinol. Metab.* 102, 2660–2669.
  48. **H. Peng.** 2017. Myokine mediated muscle-kidney crosstalk suppresses metabolic reprogramming and fibrosis in damaged kidneys, *Nat. Commun.* 8, 1493.
  49. **R.R. Chen.** 2019. Irisin attenuates angiotensin II-induced cardiac fibrosis via Nrf2 mediated inhibition of ROS/ TGFbeta1/Smad2/3 signaling axis. *Chem. Biol. Interact.* 302 11–21.